

$^{12}\text{C}(\alpha, ^8\text{Be})^8\text{Be}$ reaction in the energy range $E_\alpha = 17\text{--}33$ MeV

F. Brochard, P. Chevallier, D. Disdier, V. Rauch, G. Rudolf, and F. Scheibling
Centre de Recherches Nucléaires and Université Louis Pasteur, Strasbourg, France

(Received 12 November 1975)

Excitation functions and angular distributions for the $^{12}\text{C}(\alpha, ^8\text{Be})^8\text{Be}$ reaction were measured for $E_\alpha = 17\text{--}33$ MeV. Only broad structures were observed, except for a narrow resonance at $E_\alpha = 22.30$ MeV. Total and L -partial cross sections are deduced from the angular distributions. Below $E_\alpha = 20$ MeV no $J = 8$ resonance was found. For higher energies an $L = 8$ contribution appears, increases gradually, and becomes dominant at and above $E_\alpha = 23$ MeV. A tentative interpretation of the behavior of $^{12}\text{C}(\alpha, ^8\text{Be})^8\text{Be}$ partial cross sections is given in the framework of the Hauser-Feshbach formalism.

[NUCLEAR REACTIONS $^{12}\text{C}(\alpha, ^8\text{Be})$, $E = 17\text{--}33$ MeV, measured $\sigma(E_\alpha; \theta)$. ^{16}O]
 resonances. Natural targets.

I. INTRODUCTION

The large number of resonances identified in the work of Chevallier *et al.*¹ shows that the $^{12}\text{C}(\alpha, ^8\text{Be})^8\text{Be}$ reaction seems to be particularly well adapted to study the high energy structure of the ^{16}O nucleus. These results were confirmed by Martin and Ophel,² who studied the same reaction in the incident energy range $E_\alpha = 15\text{--}19$ MeV. They showed that in their upper energy region the highest contributing relative angular momentum for $^{12}\text{C} + \alpha$ is $L = 6$. The corresponding partial cross section was found to be dominant up to $E_\alpha = 22$ MeV simultaneously by James *et al.*³ and Brochard *et al.*⁴

The present investigation of the $^{12}\text{C}(\alpha, ^8\text{Be})^8\text{Be}$ reaction was undertaken with the principal intent of studying high spin levels in ^{16}O and especially to search for the $J^\pi = 8^+$ level belonging to a suggested 8 particle-8 hole band in this nucleus.⁵ We have measured excitation functions and angular distributions in the incident energy range $E_\alpha = 17\text{--}33$ MeV. Analysis of the results shows no evidence for a $J^\pi = 8^+$ state below $E_\alpha = 20$ MeV. Above this energy broad structures corresponding to $L = 8$ are found. The structures observed in the L -partial cross sections are compared to the predictions of a statistical Hauser-Feshbach model calculation done with a $^8\text{Be} + ^8\text{Be}$ optical potential of the type used in the description of several low energy heavy-ion reactions.

II. EXPERIMENTAL METHOD

The experiment was performed with the α^{++} beam delivered by the Strasbourg MP Tandem accelerator. The beam entered an Ortec scattering chamber through a series of 1 and 2 mm diam collima-

tors. The targets consisted of 20–50 $\mu\text{g}/\text{cm}^2$ thick, self-supporting natural carbon foils. Typical beam intensity and integrated charge were, respectively, 10–50 nA and 10 μC per data point.

A. Detection

The basic experimental method used in the present work is similar to that employed by Chevallier *et al.*¹ The ^8Be detection is achieved through a coincidence measurement between the two α particles from the ^8Be breakup. Identification of the ^8Be particles from the decay of ^{16}O is made on the basis of their kinematic characteristics. Since the $^{12}\text{C}(\alpha, ^8\text{Be})^8\text{Be}$ reaction is a two-body reaction, for a given angle the ^8Be energy is fixed and the detected ^8Be particles appear as a peak in the sum spectrum of the coincident α energies. Other possible processes give continuum shaped spectra. Two ^8Be detector systems were used in our measurements. Each system consisted of two rectangular silicon surface barrier detectors 300 μm thick, 30 mm high, 8 mm wide mounted with 4 mm vertical separation.

A computer program was used to evaluate the ^8Be detector efficiency and to optimize the geometry. It was also useful in extracting absolute cross sections. The geometry and efficiency calculations were experimentally checked by overlapping the angular range of the two ^8Be detectors. In order to match the ^8Be efficiencies of the two detectors, the distance to the target was 150 mm for the ^8Be detector placed at the forward angles and 120 mm for the one at backward angles. In this way the ^8Be effective solid angle varied by no more than a factor of 5 over the whole range of bombarding energies and measured angles (Fig. 1). This corresponded to a mean angular aperture for

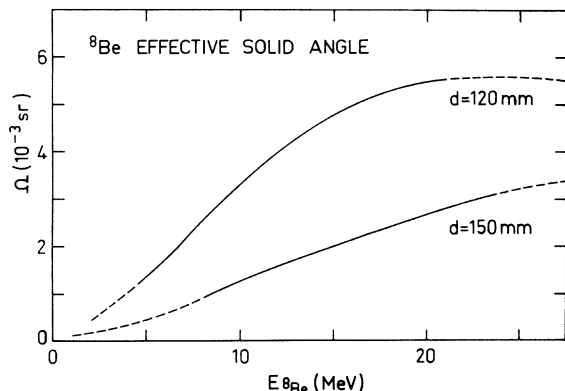


FIG. 1. Dependence on the ${}^8\text{Be}$ kinetic energy of the effective solid angle Ω of the ${}^8\text{Be}$ detectors. For the two distances indicated, the full line shows the energy range covered by each detector. The ${}^8\text{Be}$ effective solid angle, expressed in the laboratory system is defined as $\Omega = \int \epsilon d\Omega_{8\text{Be}}$, where ϵ is the probability of detecting the two α particles from the breakup of a ${}^8\text{Be}$ nucleus emitted in the solid angle $d\Omega_{8\text{Be}}$.

${}^8\text{Be}$ detection varying from two to three degrees in the c.m. system. The use of these rectangular sized detectors allowed for an efficiency improvement of a factor of about 10 with respect to that obtained by Chevallier *et al.*¹

For monitoring purposes and to get information on other reaction channels a $1000 \mu\text{m}$, 50mm^2 silicon detector was mounted 200 mm from the target at 168° to the beam axis.

To measure the dead time each preamplifier test input was fed from a pulser triggered by the digital output from a beam current integrator. In the single and coincident spectra, this pulser peak was used to measure the effective beam charge by taking into account dead time and pileup effects.

B. Data acquisition

In the sum spectrum of coincident α energies, the ${}^8\text{Be}$ ground state (g.s.) peak from the ${}^{16}\text{O}$ decay into two ${}^8\text{Be}$ particles in their ground state can be obscured by other possible processes, as for example when the ${}^8\text{Be}$ particles are emitted in their first excited state or from the ${}^8\text{Be} + \alpha$ decay of ${}^{12}\text{C}^*$. A two dimensional spectrum E_{α_1} versus E_{α_2} , as shown in Fig. 2, gives more information and allows better peak separation. The energy resolution ($\approx 4\%$) needs at least 128 channels for each dimension. This required too many channels to handle simultaneously coincidence and random spectra for two ${}^8\text{Be}$ detectors. However, based on the fact that the two dimensional spectrum is symmetrical with respect to the line $E_{\alpha_1} = E_{\alpha_2}$ (for identical gains), and that over the whole energy

range of this study the maximum energy difference between the two α particles from a ${}^8\text{Be}$ (g.s.) decay is nearly constant ($\approx 2 \text{MeV}$), the occupied memory size can be reduced by a coordinate change from E_{α_2} and E_{α_1} into $\Sigma = E_{\alpha_1} + E_{\alpha_2}$, $\Delta = |E_{\alpha_1} - E_{\alpha_2}|$. As a poor Δ resolution is sufficient, we can reduce the two dimensional spectrum to 256×4 channels without losing information, as shown in Fig. 2. The coordinate transformation is done through standard hardware electronics. It allows the storage of all desired spectra in the memory of a Hewlett-Packard 2100 computer and on-line data analysis.

III. RESULTS

Due to the fact that for the ${}^{12}\text{C}(\alpha, {}^8\text{Be} \text{ (g.s.)}) {}^8\text{Be}$ (g.s.) reaction identical particles appear in the final state, the angular distributions are symmetrical about 90° (c.m.) regardless of the reaction mechanism. The ${}^8\text{Be}$ angular distribution measurements were therefore limited to $\theta_{\text{c.m.}} \leq 90^\circ$ ($\theta_{\text{lab}} \approx 60^\circ$). Moreover, as the two final state spins are zero the angular distribution of ${}^8\text{Be}$ (g.s.) nuclei issuing from a state of spin J has the form

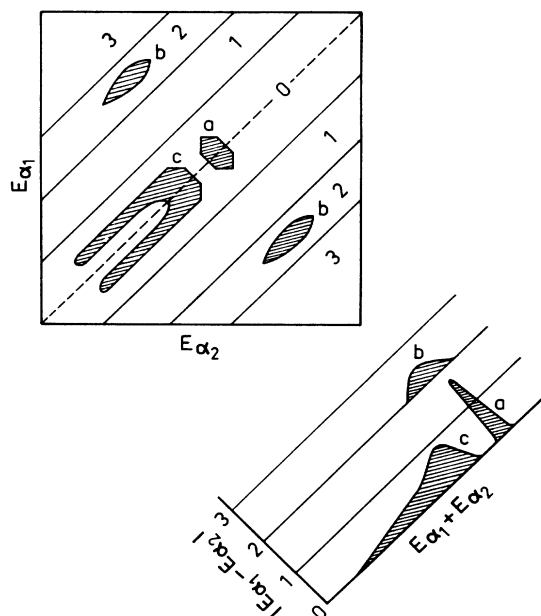


FIG. 2. Schematic representations of bidimensional spectra in the $E_{\alpha_1} \times E_{\alpha_2}$ and $|E_{\alpha_1} - E_{\alpha_2}| \times (E_{\alpha_1} + E_{\alpha_2})$ modes. The group labeled "a" corresponds to the detection of ${}^8\text{Be}$ (g.s.) nuclei from the ${}^{16}\text{O}^* \rightarrow {}^8\text{Be} \text{ (g.s.)} + {}^8\text{Be}$ (g.s.) decay; the groups labeled "b," to the detection of ${}^8\text{Be}$ (2.9 MeV) nuclei from the ${}^{16}\text{O}^* \rightarrow {}^8\text{Be} \text{ (2.9 MeV)} + {}^8\text{Be}$ (g.s.) decay. The group "c" corresponds to the detection of ${}^8\text{Be}$ (g.s.) nuclei from the preceding decay and from the ${}^{12}\text{C}^* \rightarrow {}^8\text{Be} \text{ (g.s.)} + \alpha$ decay.

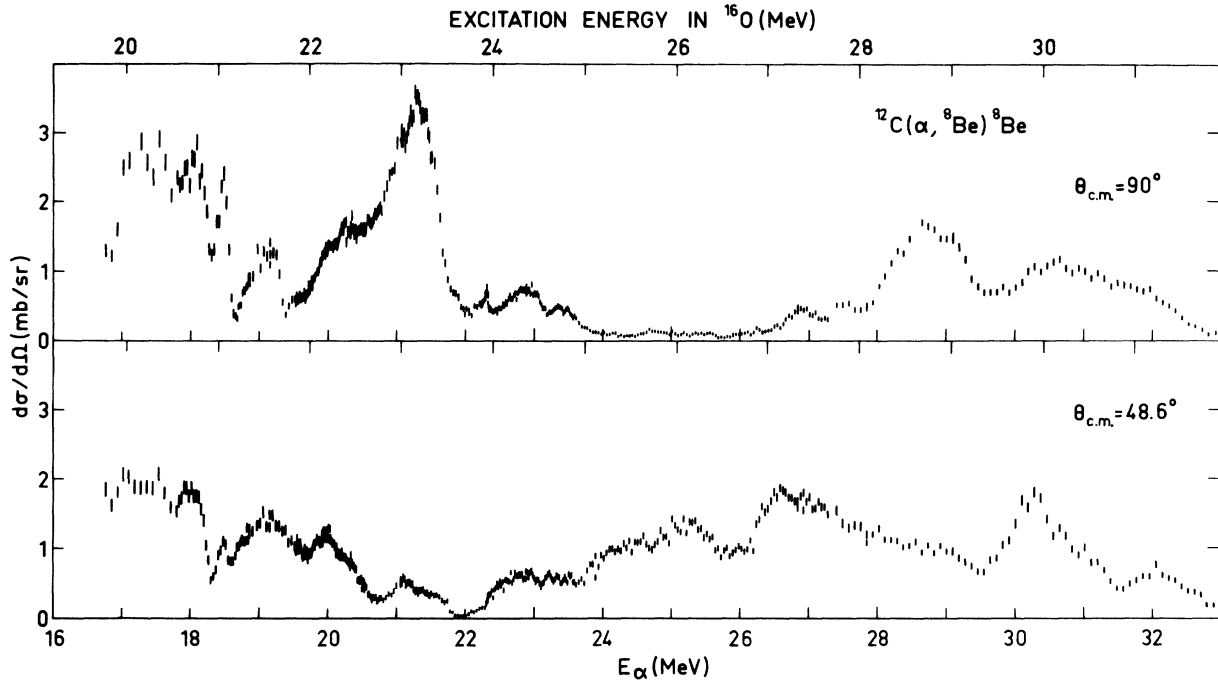


FIG. 3. Incident α -particle energy dependence at two angles of the differential cross section for the $^{12}\text{C}(\alpha, ^8\text{Be}(g.s.))\text{-}^8\text{Be}(g.s.)$ reaction.

$|P_J(\cos\theta)|^2$, where $P_J(\cos\theta)$ is a Legendre polynomial of order J . From the reaction symmetry J is restricted to even values. This implies that an excitation function at 90° (c.m.) will show any occurring resonances.

A. Excitation functions

Two excitation functions at 90° and 48.6° (c.m.) were measured simultaneously for the ^{12}C -

$(\alpha, ^8\text{Be}(g.s.))\text{-}^8\text{Be}(g.s.)$ reaction from $E_\alpha = 17\text{--}33$ MeV. Steps of 10–40 keV with thin targets were taken in some regions where narrow resonances could be expected, while 100 keV steps were used otherwise. The 48.6° angle, which corresponds to a zero of $P_6(\cos\theta)$, was chosen to identify any $J^\pi = 8^+$ level. A contribution from such a state should appear preferentially at this angle because the $L = 6$ contribution was found to be dominant up to E_α

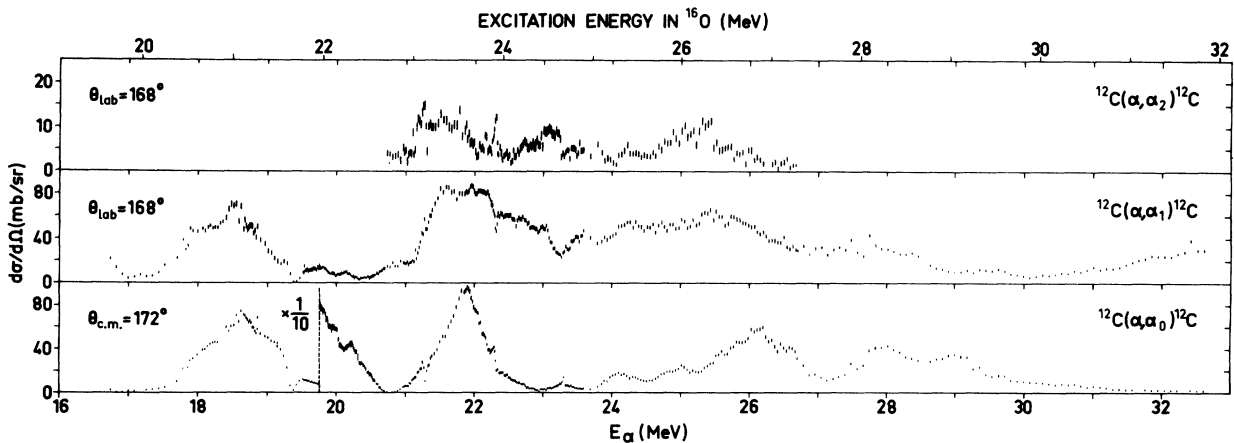


FIG. 4. Incident α -particle energy dependence at $\theta_{\text{lab}} = 168^\circ$ of the differential cross section for the $^{12}\text{C}(\alpha, \alpha')^{12}\text{C}$ reaction.

= 19 MeV (Ref. 2). The measured excitation functions are shown in Fig. 3. Due to better known geometry and target thickness estimation, taking into account carbon buildup, both absolute and relative cross sections differ slightly from our earlier work.⁴ Below $E_\alpha = 19$ MeV and at 90° (c.m.) the results are in good agreement with those of Martin and Ophel² and differ from those of James *et al.*⁶ by about 20%. Our absolute cross sections are estimated to be accurate to within 20%.

Excitation functions corresponding to the elastic and inelastic α channels from the monitor placed at 168° are represented in Fig. 4. They show no strong interchannel correlation, except for a narrow resonance at $E_\alpha = 22.30$ MeV ($E_x = 23.88$ MeV)

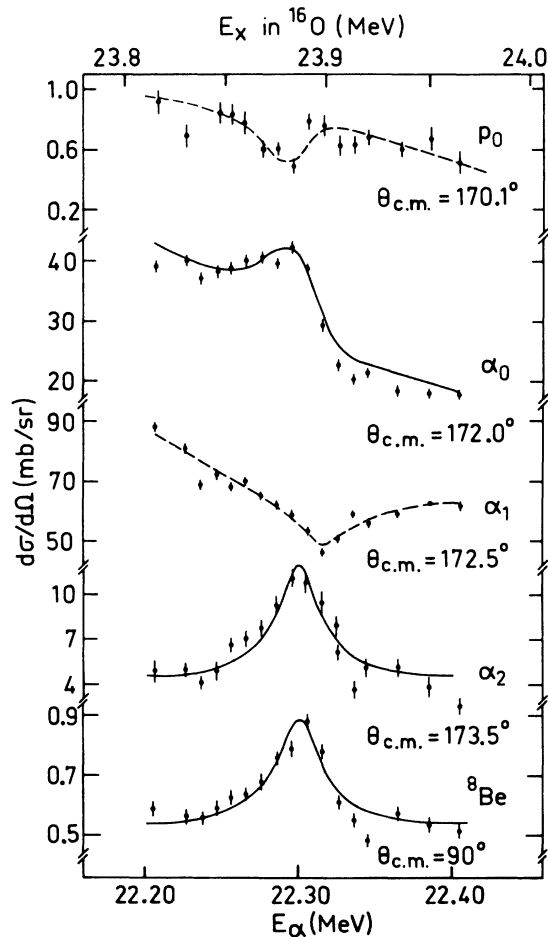


FIG. 5. Energy dependence of the differential cross section of the $^{12}\text{C} + \alpha$ reaction for several decaying channels around the $J^\pi = 6^+$ level in ^{16}O at $E_x = 23.88$ MeV. The solid lines are the results of calculations done with the parameters of Table I (see Sec. III A). The dashed lines are to guide the eye.

found previously by Hayward and Schmidt⁷ in elastic α scattering and which corresponds to a $J^\pi = 6^+$ level.⁶ The decays of this level were measured simultaneously in the $^{12}\text{C} + \alpha_0$, $^{12}\text{C} + \alpha_1$, $^{12}\text{C} + \alpha_2$, $^8\text{Be}(\text{g.s.}) + ^8\text{Be}(\text{g.s.})$, and $^{15}\text{N} + p$ channels. All the resulting excitation functions show a resonant behavior (Fig. 5). It should be pointed out that this level has both a proton and a ^8Be width. Such a situation has already been observed for a $J^\pi = 4^+$ state excited at $E_\alpha = 14.52$ MeV (Ref. 1). The analysis of the elastic scattering data (Fig. 5) using the phase shifts determined by Carter⁹ leads to the ratio $\Gamma_{\alpha_0}/\Gamma = 0.06 \pm 0.02$ for the $J^\pi = 6^+$ level. If we describe in a crude way the resonance at $E_\alpha = 22.30$ MeV in the $^{12}\text{C} + \alpha_2$ and $^8\text{Be}(\text{g.s.}) + ^8\text{Be}(\text{g.s.})$ channels through Breit-Wigner shapes, we can deduce approximate values for $\Gamma_{^8\text{Be}}$ and Γ_{α_2} by taking into account the theoretical forms of the angular distributions. The results for the $J^\pi = 6^+$ level are given in Table I.

B. Angular distribution

Since our earlier work⁴ most of the $^8\text{Be}(\text{g.s.})$ angular distribution measurements were extended to 10° (lab) ($\approx 17^\circ$ c.m.). The measured angular distributions are shown in Fig. 6. Their shapes vary slowly with incident energy even when the excitation functions (Fig. 3) show resonancelike structure. The number of minima between 0° and 90° increases from 3 to 4 while their positions shift from the zero of $P_6(\cos\theta)$ to those of $P_8(\cos\theta)$ for increasing bombarding energies.

Despite the low efficiency for detecting $^8\text{Be}(2.9$ MeV) (^8Be nuclei in their first excited state) which was about 300 times smaller than that for detecting $^8\text{Be}(\text{g.s.})$, it was still possible to measure some such angular distributions. In calculating the efficiency for the $^8\text{Be}(2.9$ MeV) detection, we assumed an isotropic correlation between the $^8\text{Be}(2.9$ MeV) and the emitted α particles. In the energy range of the measurements $E_\alpha = 19.1$ – 22.3 MeV, large cross sections are observed as can be seen in Fig. 7. Some angular distributions are strongly peaked near 90° (c.m.) and, as with the decay to $^8\text{Be}(\text{g.s.})$, show a weak energy dependence.

TABLE I. Parameters of the $J^\pi = 6^+$ level at $E_x = 23.88$ MeV in ^{16}O .

E_r (MeV)	Γ (keV)	$\Gamma_{^8\text{Be}}$ (keV)	Γ_{α_0} (keV)	Γ_{α_2} (keV)
22.295 ± 0.015	25 ± 5	≈ 3.5	1.5 ± 0.5	≈ 6
22.309 ± 0.007^a	26 ± 4^a			

^a Reference 6.

IV. ANALYSIS

For the $^{12}\text{C}(\alpha, ^8\text{Be}(\text{g.s.}))^8\text{Be}(\text{g.s.})$ reaction a general expression for the differential cross section is⁸

$$\frac{d\sigma}{d\Omega}(E, \theta) = \left| \sum_{\text{even } L}^{L_{\text{max}}} \alpha_L(E) (2L+1)^{1/2} P_L(\cos\theta) \right|^2, \quad (4.1)$$

where the $\alpha_L(E)$ are complex numbers.

From (4.1) the total cross section is

$$\sigma(E) = 4\pi \sum_{\text{even } L}^{L_{\text{max}}} |\alpha_L(E)|^2. \quad (4.2)$$

In this decomposition, each term represents the L -partial cross section.

The differential cross section can also be expressed linearly in terms of even Legendre polynomials. However, as the coefficients of this decomposition have no unique interpretation in terms of L -partial cross sections (except for the highest L value), formula (4.1) was used in a nonlinear

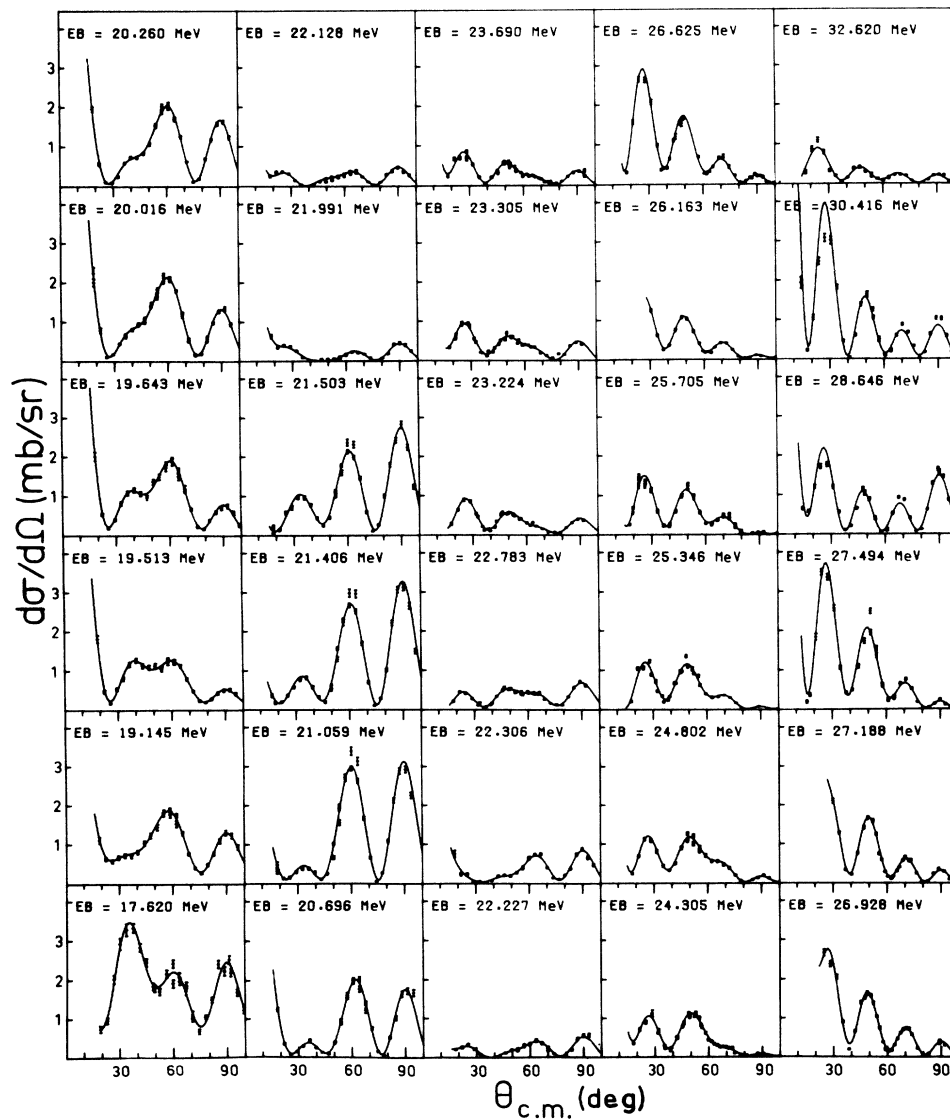


FIG. 6. Angular distributions in the c.m. observed at several bombarding energies for the $^{12}\text{C}(\alpha, ^8\text{Be}(\text{g.s.}))^8\text{Be}(\text{g.s.})$ reaction. The solid lines are the results of a nonlinear fit to the data with formula (4.1) (see Sec. IV). Here, EB stands for the α bombarding energy.

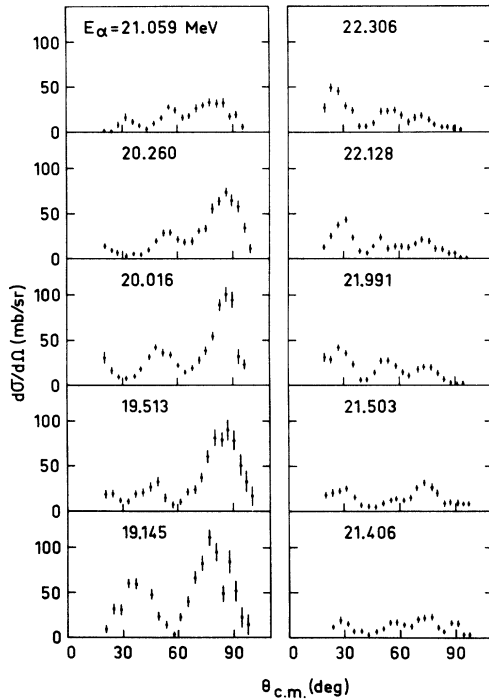


FIG. 7. Angular distributions in the c.m. measured at several bombarding energies for the $^{12}\text{C}(\alpha, ^8\text{Be} (2.9 \text{ MeV}))^8\text{Be}$ (g.s.) reaction.

fitting program.

In Fig. 8, we show the total and partial cross sections deduced from the angular distributions measured in this work (Fig. 6), in the work of Chevallier *et al.*,¹ and that of Martin and Ophel.² Several sets of $\alpha_L(E)$ values corresponding to about the same minimum χ^2 value were obtained for each angular distribution. The origin of this multiplicity arises from the fact that there is at least one ambiguity in the formula (4.1) for $L < L_{\text{max}}$ and also because it was not possible to measure data in the very forward angular region. For each measured distribution we have indicated the extreme values for the total and L -partial cross sections by a vertical bar in Fig. 8. These bars correspond to the $\alpha_L(E)$ values giving the lowest χ^2 values. The importance of the forward angle measurements can be seen particularly in the results deduced from the work of Martin and Ophel² (vertical dashed bars), where the angular distributions were given only for $\theta_{\text{c.m.}} > 35^\circ$.

At least three different L values were necessary to explain each measured angular distribution. This excludes the possibility of a one level interpretation of the data. The $\alpha_L(E)$ coefficient corresponding to the highest L value always becomes

dominant while the others are involved mainly through cross terms. The phases of these coefficients are found to be nearly constant. Even when passing through structures no discontinuity appeared.

V. DISCUSSION

We consider here our data together with previous results¹ obtained in the incident energy range $E_\alpha = 12$ –19 MeV. From a similar decomposition of the cross sections, resonances for spins $J = 2$ –6 were observed to lie approximately on an $J(J+1)$ line.¹ This suggested the existence of an ^{16}O rotational band with a very high moment of inertia, interpreted later as an 8 particle-8 hole band.⁵ One purpose of this study was to locate its $J^\pi = 8^+$ member.

A. Search for a $J^\pi = 8^+$ level

The excitation functions measured in the energy region $E_\alpha = 18.5$ –21 MeV in 5 to 20 keV steps failed to show evidence for such a state. The same conclusion is reached after a search for an $L = 8$ term in the angular distributions. Up to $E_\alpha = 20$ MeV no evidence for such a term is found. About this energy, a weak but slowly increasing $L = 8$ component appears and becomes dominant at $E_\alpha = 23$ MeV (Fig. 8). Above $E_\alpha = 27$ MeV the nonlinear fit indicates the presence of an $L = 10$ component. This implies that if a $J^\pi = 8^+$ level belonging to the predicted 8 particle-8 hole band exists below $E_\alpha = 20$ MeV, it would have a very different width from the other members of the band. One possibility to explain this difference in width is that the formation of this level might be inhibited either in the entrance or outgoing channels.

To test this hypothesis we report in Fig. 8 the energies corresponding to the grazing angular momentum given by the semiclassical formula

$$L(L+1) = k^2 R^2 (1 - 2\eta/kR), \quad (5.1)$$

where $R = R_0(A_1^{1/3} + A_2^{1/3})$, and k and η are, respectively, the wave number and the Sommerfeld parameter for the considered channel. In the entrance channel ($R_0 = 1.4$ fm) the possibility of an inhibition for $L = 8$ is important below $E_\alpha = 20$ MeV. In the ^8Be (g.s.) + ^8Be (g.s.) exit channel, the observed structures appear for each L value about 5 MeV below energies calculated with formula (5.1) and $R_0 = 1.4$ fm. However, the agreement becomes quite satisfactory (Fig. 8) if we use a larger radius parameter $R_0 = 1.8$ fm, which might take better account of the loose α -cluster structure of the ^8Be nucleus¹⁰ and of a 4α linear configuration breakup of ^{16}O into two ^8Be . Hence, no particular inhibition can be expected in the outgoing channel.

B. Reaction mechanism

The broad structures observed for $L=0-8$ (Fig. 8) are characterized by their appearance near the energies corresponding to the grazing angular momentum for the outgoing channel and by their energy localization for each L value. This behavior, where a single partial wave dominates within a restricted range of energy, is typical of a surface mechanism and can be explained by the formation

of quasimolecular states. This hypothesis is strengthened by the low cross sections for a direct mechanism estimated by extrapolation from higher incident energy results¹¹ ($E_\alpha = 65$ MeV). These cross sections are about an order of magnitude lower than the observed ones.

A similar situation where resonancelike structures are observed near the Coulomb barrier is encountered in the study of reactions like $^{12}\text{C} + ^{12}\text{C}$

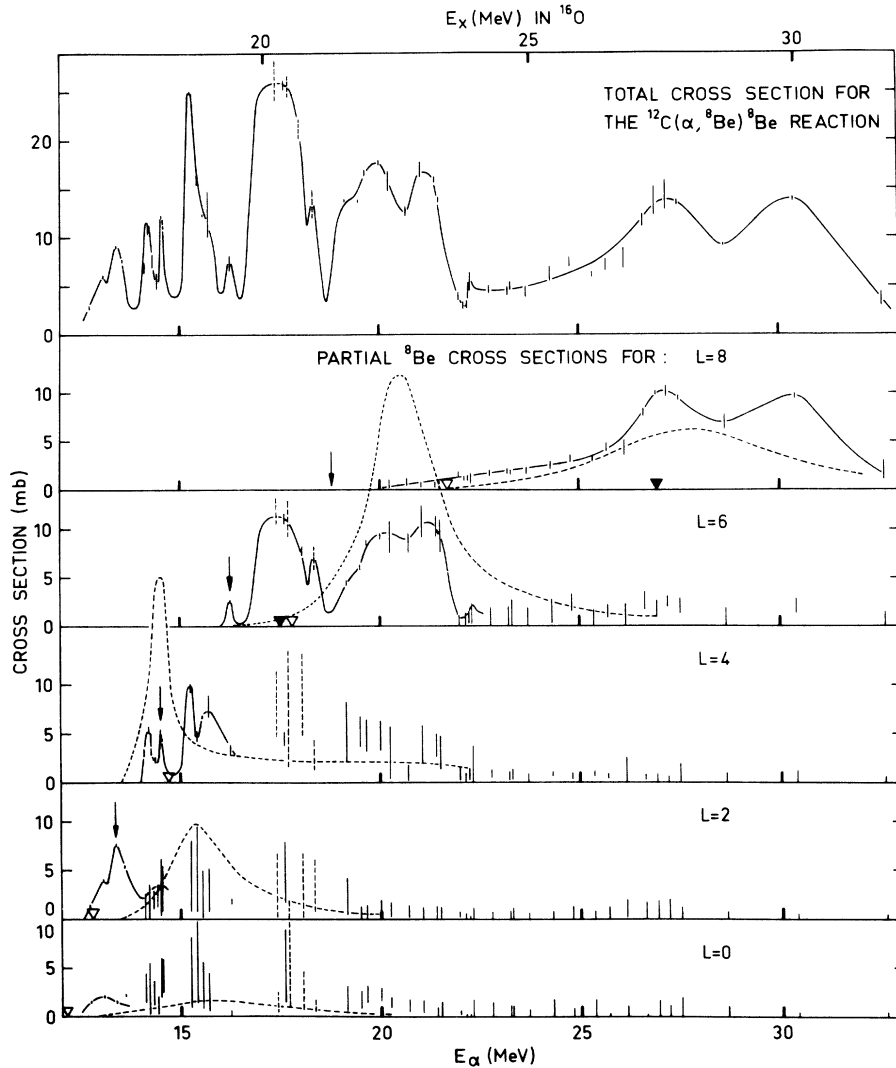


FIG. 8. Total and L -partial cross sections of the $^{12}\text{C}(\alpha, ^8\text{Be}(\text{g.s.}))^8\text{Be}(\text{g.s.})$ reaction for $E_\alpha = 12-33$ MeV. The solid lines are to guide the eye and correspond to the general trend of the measured differential cross sections. The dashed lines correspond to the results of a statistical Hauser-Feshbach compound nuclear calculation done with the parameters given in Table II. The solid and open triangles represent, respectively, the energies corresponding to the grazing angular momentum (see Sec. VA) for the entrance and outgoing channels. The arrows show the position of the $J^\pi = 2^+ - 6^+$ levels of the 8 particle-8 hole band (Ref. 5) and the predicted position of the $J^\pi = 8^+$ member of this band assuming a $J(J+1)$ rule. The solid bars correspond to the decomposition of the angular distributions measured in this work and by Chevallier *et al.* (Ref. 1). The dashed bars correspond to the decomposition of the measurements of Martin and Ophel (Ref. 2).

TABLE II. Optical model parameters used in the Hauser-Feshbach calculation. The level density equations and the related parameters are those defined by Gilbert and Cameron (Ref. 19). The forms of the potentials are defined in Ref. 20.

Channel	U (MeV)	R_U^a (fm)	a_U (fm)	W^b (MeV)	R_W^a (fm)	a_W (fm)	$V_{s.o.}$ (MeV)	$R_{s.o.}^a$ (fm)	$a_{s.o.}$ (fm)	E_c^c (MeV)
$^{15}\text{N}+p$	50.9 ^d	1.25	0.65	13.5	1.25	0.47	5.5	1.04	0.65	9.16
$^{15}\text{O}+n$	48 ^d	1.25	0.65	8.5	1.25	0.98	5.5	1.25	0.65	9.61
$^{14}\text{N}+d$	88 ^d	1.15	0.81	12	1.34	0.68				9.71
$^{13}\text{C}+^3\text{He}$	158 ^e	0.93	0.81	6.8	2.25	0.65	6	0.93	0.81	9.50
$^{13}\text{N}+t$	150 ^d	1.24	0.68	20	1.45	0.84				8.92
$^{12}\text{C}+\alpha$	185 ^d	1.4	0.52	25	1.4	0.52				16.11
$^8\text{Be}+^8\text{Be}$	10.6 ^f	1.4	0.45	0.1	1.4	0.45				16.93

^a $R = R_U A_2^{1/3}$ except in the $^8\text{Be} + ^8\text{Be}$ channel where $R = R_U (A_1^{1/3} + A_2^{1/3})$ (A_1 and A_2 are, respectively, the mass number of the light and heavy particles in the considered channel). The Coulomb radius is equal to the radius of the real well.

^b The imaginary well is of the surface type for the $^{14}\text{N}+d$ and $^{15}\text{N}+p$ channels, of the Gaussian type in the $^{15}\text{O}+n$ channel, and are of the volume type in all others.

^c Energy above which continuum level densities are used.

^d Reference 20.

^e Reference 23.

^f The $^8\text{Be} + ^8\text{Be}$ optical potential is adapted from the one used by Maher *et al.* (Ref. 21).

or $^{12}\text{C} + ^{16}\text{O}$ (Ref. 12). Most of the models developed to explain such behavior are based on two different hypotheses. The first assumes the formation of α -particle molecules.^{13,14} The conditions¹⁴ for the existence of these molecules are also fulfilled for the $^{12}\text{C}(\alpha, ^8\text{Be}(\text{g.s.}))^8\text{Be}(\text{g.s.})$ reaction. However, the lack of apparent correlations with other exit channels like $^{12}\text{C} + \alpha_0$, $^{12}\text{C} + \alpha_1$, and $^{12}\text{C} + \alpha_2$ disfavors this hypothesis in our case. The second possibility is based on the creation of quasimolecular states. Several tentative interpretations to reproduce the observed resonancelike structures have been done with optical model calculations using very shallow potentials.¹⁵⁻¹⁸ We have made such an interpretation for the $^{12}\text{C}(\alpha, ^8\text{Be}(\text{g.s.}))^8\text{Be}(\text{g.s.})$ reaction by using a statistical Hauser-Feshbach model calculation with the parameters given in Table II. This calculation is not well adapted to all the incident energies of this study due to the small level densities and number of open channels in the ^{16}O nucleus for lower excitation energies. The heavy-ion optical potential used to describe the $^8\text{Be} + ^8\text{Be}$ scattering must have a very small imaginary part in order to reproduce the observed structures which are only produced by the transmission coefficients relevant to the outgoing channel. In Fig. 8 the calculated curves (dashed lines) are compared to the experimental data. The similitude between the broad predicted structures and the behavior of the experimental cross sections is in surprising

agreement with the nuclear molecule hypothesis. Recent results obtained for the $^{16}\text{O}(\alpha, ^8\text{Be})^{12}\text{C}$ reaction²² show a different behavior which could imply that the structures are due to the simultaneous presence of two ^8Be nuclei.

VI. CONCLUSION

In the energy range $E_\alpha = 17-33$ MeV of this study only one narrow resonance, corresponding to a $J^\pi = 6^+$ level, is found at $E_\alpha = 22.30$ MeV. Below $E_\alpha = 20$ MeV the existence of a $J^\pi = 8^+$ level cannot be definitively ruled out, as it may be possible that the limited amount of angular momentum in the entrance channel inhibits the formation of such a level.

The analysis of the measured angular distributions allows the extraction of L -partial cross sections. The broad resonant structures observed near the Coulomb barrier in the outgoing channel are characterized by the successive appearance of $L = 0$ to $L = 8$ components and the energy localization of these structures for each L value. They are related to the exit channel and may be attributed to the formation of nuclear molecules. However, the different behavior observed recently²² would make it interesting to study other $(\alpha, ^8\text{Be})$ reactions where $4n$ nuclei are involved.

We wish to thank Dr. A. Pape for critically reading the manuscript.

- ¹P. Chevallier, F. Scheibling, G. Goldring, I. Plessler, and M. W. Sachs, *Phys. Rev.* **160**, 827 (1967).
- ²P. Martin and T. R. Ophel, *Nucl. Phys.* **A194**, 491 (1972).
- ³D. R. James, J. L. Artz, M. B. Greenfield, and N. R. Fletcher, in *Proceedings of the International Conference on Nuclear Physics, Munich, 1973*, edited by J. de Boer and H. J. Mang (North Holland, Amsterdam/American Elsevier, New York, 1973), Vol. I, p. 164.
- ⁴F. Brochard, P. Chevallier, D. Disdier, G. Rudolf, and F. Scheibling, in *Proceedings of the International Conference on Nuclear Physics, Munich, 1973* (see Ref. 3), Vol. I, p. 204.
- ⁵Y. Abgrall, G. Baron, E. Caurier, and G. Monsonégo, *Phys. Lett.* **26B**, 53 (1967).
- ⁶D. R. James, J. L. Artz, M. B. Greenfield, and N. R. Fletcher, *Nucl. Phys.* **A227**, 349 (1974).
- ⁷T. D. Hayward and F. H. Schmidt, *Phys. Rev. C* **1**, 923 (1970).
- ⁸A. M. Lane and R. G. Thomas, *Rev. Mod. Phys.* **30**, 257 (1958).
- ⁹E. B. Carter, *Phys. Lett.* **27B**, 202 (1968).
- ¹⁰A. Arima, K. Kubodera, H. Horiuchi, and N. Takigawa, in *Advances in Nuclear Physics*, edited by M. Baranger and E. Vogt (Plenum, New York, 1972), Vol. V, p. 345.
- ¹¹G. J. Wozniak, N. A. Jelley, and J. Cerny, *Phys. Rev. Lett.* **31**, 607 (1973).
- ¹²R. H. Siemssen, in *Nuclear Spectroscopy and Reactions*, edited by J. Cerny (Academic, New York, 1972), Part B, p. 233.
- ¹³G. J. Michaud and E. W. Vogt, *Phys. Rev. C* **5**, 350 (1972).
- ¹⁴H. Voit, P. Dück, W. Galster, E. Haindl, G. Hartmann, H. D. Helb, F. Siller, and G. Ischenko, *Phys. Rev. C* **10**, 1331 (1974).
- ¹⁵B. N. Nagorcka and T. O. Newton, *Phys. Lett.* **41B**, 34 (1972).
- ¹⁶B. Imanishi, *Nucl. Phys.* **A125**, 33 (1969).
- ¹⁷E. Vogt and H. McManus, *Phys. Rev. Lett.* **4**, 518 (1960).
- ¹⁸K. W. McVoy, *Phys. Rev. C* **3**, 1104 (1971).
- ¹⁹A. Gilbert and A. G. W. Cameron, *Can. J. Phys.* **43**, 1446 (1965).
- ²⁰N. Austern, in *Direct Nuclear Reaction Theories*, edited by R. E. Marshak (Wiley, New York, 1970), p. 109.
- ²¹J. V. Maher, M. W. Sachs, R. H. Siemssen, A. Weidinger, and D. A. Bromley, *Phys. Rev.* **188**, 1665 (1969).
- ²²G. Rudolf, Ph.D. thesis, Strasbourg, 1975 (unpublished).
- ²³R. W. Zurmühle and C. M. Fou, *Nucl. Phys.* **A129**, 502 (1969).